MEASUREMENT OF THE EFFECT OF POWERFUL ELECTRON BEAMS ON BARRIERS

A. A. Ignatov, A. A. Provalov,
B. D. Khristoforov, and O. G. Chernov

UDC 536.422.1

In connection with the possibility of using powerful electron beams for various technological purposes [1-6] and the excavation of mine workings [7], a study was made of the effect of powerful electron beams on metal and dielectric barriers. Measurements were made of brightness temperature and departure velocity of the vapor produced, and of the thermal flux and mechanical loading on the barriers when acted upon by electron beams with currents to 40 kA and electron energies of 60-100 keV.

The experiments were performed with accelerators having the following parameters [8, 9]; beam current, up to 40 kA, accelerating voltage, 60-100 kV; beam diameter, up to 3 cm; voltage pulse durations and beam energies of 0.2 and 1.5 μsec, 180 and 1300 J. The barriers to be irradiated were placed in the accelerator drift tube, which was evacuated to 10^{-6} mm Hg.

Pulse energy was determined from current oscillograms at the target and the applied accelerating voltage, and also from the degree of heating of copper calorimeters, as measured by thermocouples. Beams energy density decreased from the center to the edges. Calorimeters with input orifices varying from 5 to 60 mm in diameter were used to determine beam energy distribution across the section. Due to evaporation of the calorimeter walls and removal of portions of the evaporated material, the calorimetric measurements were lower in value than the electrical measurements, the divergence increasing with increase in beam energy, but not exceeding 20% [10].

The measured energy density in the beam with calorimeter input orifice diameters of 5, 10, 20, 30 mm comprised 110, 65, 30, 16 J/cm^2 with the accelerator of [8] and 260, 120, 110, 100 J/cm^2 with the accelerator of [9].

Measurements of mechanical momentum were made with an MID membrane momentum-meter or a PIM piezoelectric momentum meter. The MID contains an elastic membrane, the deflection of which by the beam is proportional to the beam momentum. The deflection is determined by the distortion of a lead crusher gauge located beneath the membrane. Membranes of steel, Dural, and Plexiglas, with diameters from 10 to 30 mm were used. Targets of other materials were glued to the membrane with epoxy resin.

Measurement uncertainties developed because of thermoelastic deformations of the membranes and changes in their elastic characteristics due to heating and annealing, and also because of deviation of the beam center from the center of the membrane. With careful monitoring of the membrane characteristics the measurement error did not exceed 15%.

The PIM piezoelectric momentum meter contains a removable target made of the material to be studied, mounted on a three-bracket elastic element. When the beam strikes the target the momentum transferred excites oscillations of the elastic element, which are converted to electrical signals by TsTS-19 piezotransducers installed below the brackets. The emf recorded on the oscilloscope varies at the elastic-element oscillation frequency, and the amplitude is proportional to the momentum acting. The pulse magnitude can be determined from any successive signal peaks, allowing pulse registration after pulse completion in the presence of much interference. Thermoelastic stresses and deformations and beam deviations from the target center have no effect on device operation so that the uncertainty of standard measurements does not exceed 10%. Device sensitivity is up to 0.5 V × 1000 pF/dyn · sec.

Moscow. Translated from Zhurnal Prikladnoi Mekhaniki i Tekhnicheskoi Fiziki, No. 5, pp. 3-7, September-October, 1979. Original article submitted October 26, 1978.

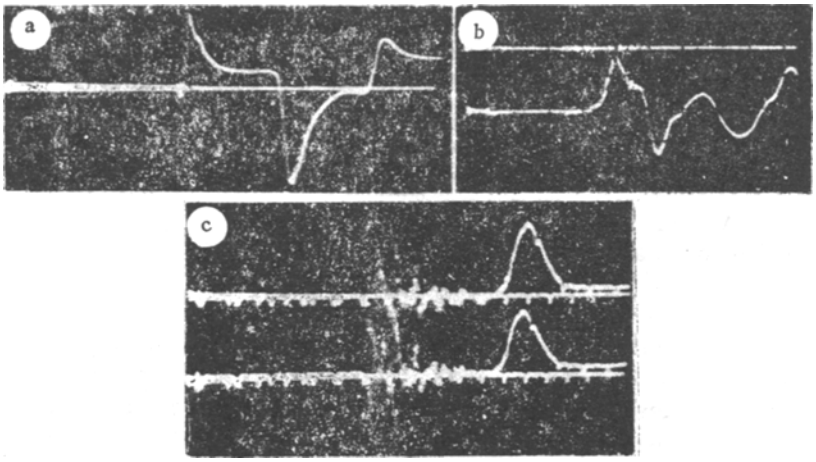

Fig. 1

After beam application to the target surface, traces of erosion due to evaporation and melting were observed. The central (usually circular) region is related basically to departure of evaporated material, while the peripheral area was produced by spattering of melted material. Outside these regions the metallic targets showed tempering colors. The dielectric targets, quartz, TsTS, and Plexiglas, were destroyed by cracking and splitting.

With increase in beam energy Q the measured values of transferred momentum I increase, although the ratios I/Q using the accelerators of [8, 9] are close in value, and coincide for lead and silver near 10 dyn • sec/J.

Mass removal m was determined by weighing the target before and after beam action. With increase in target radius, mass removal decreased due to deposition of melted particles on the targets themselves, which was especially marked for the steel and copper targets. The amounts of mass removed are approximately proportional to the beam energy absorbed and depend weakly on flux density and electron energy. In D16T Dural and aluminum, which had the highest heats of sublimation, mass removal was significantly greater than in steel and copper, since due to the low melting point a significant amount of aluminum and D16T were removed in liquid form.

Measurements on an aluminum target 40 mm in diameter, composed of 64 elements, showed that mass removal per unit area is maximal in the center and decreases toward the edges of the irradiated spot, corresponding approximately to the energy distribution over spot area. Therefore, the ratio m/Q for the various target elements remains practically constant.

Characteristic values of mass removed with the accelerator of [8] and 30-mm diameter targets of steel, Dural, lead, silver, quartz, and Plexiglas were near 20, 70, 200, 70, 40, 190 μg/J. With the accelerator of [9] m/Q values were somewhat lower than with the other device [8], since with increase in the duration of the interaction a larger fraction of beam energy is absorbed in vapor.

The time dependence of pressure was measured by end-window piezoelectric sensors operating in the current generator regime with time resolution down to 10^{-8} sec and total time registriation to 2 μsec. The outer surface of the sensitive element made of TsTS-29 piezoceramic or quartz, 30 mm in diameter, upon which the target was mounted, was subjected to beam action. The signal was taken from the inner (surrounded by a guard ring) measurement electrode, the diameter of which was 20, 15, 10, 6, or 4 mm, for the various sensitive elements, permitting measurement of average pressure as a function of time on a target equal in area to the measurement electrode area. Recording was done with an S-1-26 oscilloscope. Targets used were silver, copper, aluminum, lead, and epoxy. The TsTS-19 piezoelements operated reliabily in the accelerator of [8], but with the device of [9] they could not be used for pressure recording because of the high intensity of braking x radiation. The piezomodule was changed markedly by beam action. Use of targets with a thickness greater than the x-ray mean free path length permitted recording of pressure measurements, but led to reduced values due to shock wave damping in the depths of the target. Therefore, quartz piezoelements were used with the accelerator of [9], since these are not sensitive to x radiation.

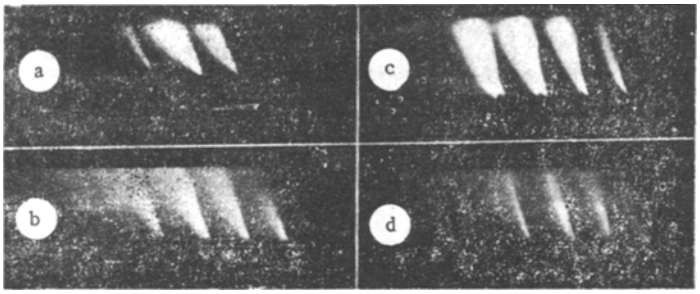

Fig. 2

TABLE 1

Material	D16T		Steel		Lead		Plexiglas	
Accelerator	[8]	[9]	[8]	[9]	[8]	[9]	[8]	[9]
$T_m 10^{-3}$ °K	9,5	45	14,5	60	10	35	6.5	10
v_m, km/sec	10	10	10	10	8	8	9	—
ρ, 10^3 g/cm^3	—	2,9	—	2,5	—	16	—	—

Figure 1a–c shows characteristic oscillograms of pressure for beam action on silver (p_m = 2550 atm [8]), lead (p_m = 1460 atm [8]), and aluminum (p_m = 700 atm [9]). Aside from the basic shock wave, there develops a train of waves reflected from the piezoelement surface. The maximum pressure p_m increases with increase in electron flux density, and the pressure maximum is found at a time close to the maximum irradiation power. In silver, for change in flux density from 180 to 670 mW/cm^2 the maximum pressure increases from 1500 to 4200 atm, while for copper over the range 180–470 mW/cm^2 the pressure increases from 730 to 1900 atm, and in lead for 50–225 mW/cm^2 from 500 to 1500 atm. In aluminum and epoxide for a charge density 170 mW/cm^2 the maximum pressure is 850 and 1460 atm, respectively.

The total mechanical momentum was determined from the pressure oscillograms only for the accelerator of [8], because with the accelerator of [9] the sensor recording time of 2 μsec was insufficient, since target loading by vapor pressure extends for a time approximately an order of magnitude longer than the beam action time.

Measurement of residual heat in the target was performed simultaneously by 2 or 3 copper-Constantan thermocouples with a thermal emf of about 41.6 μV/deg C with recording on an N-117 loop oscilloscope. The thermocouples were inserted in the targets subjected to beam action.

Target heating is basically related to braking of electrons in deep layers from which no material is ejected, to radiation from the plasma cloud above the target, and to deposition of melted material beyond the limits of the irradiated spot. The influence of the latter effect increases with target size.

Residual heat measurements in metals with the accelerator of [9] and a beam energy of 860 J showed that with the MID device and a face diameter of 65 mm the residual heat values in steel, aluminum, and lead comprise 340, 310, and 280 J, or about 35–40% of the total beam energy.

With the apparatus of [8] and a target diameter of 30 mm in steel, Dural, and quartz, the residual heats comprised 78, 67, and 50% of the beam energy. Usually more heat is transferred to refractory materials than to low-melting-point materials.

The pattern of luminous vapor ejection was recorded by ZhFR and SFR-2M cameras. The latter camera produced a picture viewed through five raster slits 0.02 mm in width, normal to the target surface. A magnification of about 1.3 was achieved with a special lens attachment. Time resolution was about 0.03 μsec. Use of the raster technique permitted determination of the flare form at various moments in time. Brightness temperature of the vapors was determined by comparing film density with reference density marks obtained by photographing a standard ÉV-39 light source with brightness temperature 39000 ± 2000°C through a step attenuator.

TABLE 2

Material	Steel		Aluminum		Lead	
Evaporation energy	75 J	9%	185 J	22%	83 J	10%
Vapor kinetic energy	130 J	15%	85 J	10%	43 J	5%
Residual heat	340 J	40%	310 J	36%	280 J	33%
Internal vapor energy with consideration of ionization	205 J	24%	250 J	29%	310 J	36%
Total energy expenditure	750 J	88%	828 J	96%	716 J	83%

Photograms of vapor ejection with the accelerator of [8] are shown in Fig. 2 (image scan right to left, magnification 1.3, scan rate 3 mm/μsec, a) silver; b) lead; c) steel; d) aluminum). The general pattern for all the metals is approximately the same. All photographs show an outer zone brightest of all (the boundary of vapor motion), which is detached from the target edge. The brightness temperature of the vapor with the accelerator of [9] is significantly higher than with the accelerator of [8], because of the higher beam energy, but the ejection velocities v_m are practically the same. The mean vapor density $\bar{\rho}$ at the end of beam action was determined from the measured vapor volume and the mass removed. The pattern of vapor removal from dielectrics differs significantly from that for metals. Analysis of the photographs shows that evaporation begins at the very commencement of beam action and further beam absorption occurs in the vapor. The vapor zone of maximum brightness moves away from the target with time, but always remains at the leading edge of the vapor. The vapor temperature distribution over height correlates with electron energy liberation curves.

At the completion of beam action the vapor temperature at the target is several times lower than the maximum T_m. Some results are given in Table 1.

The measurements performed permit estimation of beam energy expenditure for the various processes which occur (Table 2).

The energy balance over averaged results of the experiments agrees well with measurements of the beam energy Q = 860 J.

The authors express their gratitude to D. V. Iremashvili and his laboratory co-workers T. A. Osepashvili, P. I. Kakuchaya, and V. D. Popov for making it possible to use the accelerators.

LITERATURE CITED

1. C. Woodruff, "Numerical calculation of ring deformation with pulsed electron beam action," Prikl. Mekh., No. 4 (1971).
2. Woodruff, Giedt, and Hess, "Surface melting, splintering, and stress development in metals under pulsed heating," Prikl. Mekh., No. 2 (1971).
3. M. Farber, I. Robin, and R. Srevastava, "High-power electron beam deposition studies on aluminum and graphite," J. Appl. Phys., 43, No. 8 (1972).
4. Bogolyubskii and Gerasimov, "Heating of thin foils by a high-current electron beam," Pisma Zh. Eksp. Teor. Fiz., 24, No. 4 (1976).
5. V. A. Artemov, M. A. Vlasov, O. A. Malafeev, A. V. Reder, A. V. Rykhlov, and V. A. Safonov, "Experimental study of nonstationary metal evaporation under action of an electron beam," Zh. Tekh. Fiz., 48, No. 1 (1978).
6. V. A. Artemov and M. A. Vlasov, "Nonstationary evaporation in the interaction of an electron beam with metal," Zh. Tekh. Fiz., 48, No. 1 (1978).
7. E. Fogelson, "Advanced fragmentation techniques," Adv. Rock. Mech., 1, Pt. BDC (1974).
8. D. V. Iremashvili, S. V. Kuril'nikov, N. I. Leont'ev, and T. A. Osepashvili, "High-current plasma electron beam with pulse current of 50 kA," Pisma Zh. Eksp. Teor. Fiz., 17, No. 1 (1972).
9. D. V. Iremashvili, P. I. Kakuchaya, and T. A. Osepashvili, "Formation of a high-intensity beam of μsec duration," Pisma Zh. Eksp. Teor. Fiz., 20, No. 11 (1975).
10. D. V. Iremashvili, P. I. Kakuchaya, T. A. Osepashvili, and A. N. Kuz'min, "Some peculiarities in calorimetry of high-intensity electron beams with energies of 10^5 eV," in: Design and Practical Application of Electron Accelerators [in Russian], Tomsk State Univ. (1975).